

On Third-Order Limiter Functions for Finite Volume Methods

Birte SCHMIDTMANN^{a,*}, Rémi ABGRALL^{b)}, and Manuel TORRILHON^{a)}

ABSTRACT. In this article, we propose a finite volume limiter function for a reconstruction on the three-point stencil. Compared to classical limiter functions in the MUSCL framework, which yield 2nd-order accuracy, the new limiter is 3rd-order accurate for smooth solution. In an earlier work, such a 3rd-order limiter function was proposed and showed successful results [2]. However, it came with unspecified parameters. We close this gap by giving information on these parameters.

1. Introduction

We consider the numerical approximation of hyperbolic conservation laws of the form

$$\begin{aligned} (1a) \quad & u_t + (f(u))_x = 0, \\ (1b) \quad & u(x, 0) = u_0(x), \end{aligned}$$

where $u = (u_1, \dots, u_s)^T$ and the Jacobian matrix $A(u) = \partial f / \partial u$ has s real eigenvalues. In this work, we restrict our discussion to the scalar 1D case $s = 1$. We further assume $u_0(x)$ to be either periodic or to have compact support.

On a regular computational grid with space intervals of size Δx , let x_i denote the position of the cell centers. The control cells are defined by $C_i = [x_{i-1/2}, x_{i+1/2}]$, where $x_{i\pm 1} = x_i \pm \Delta x$.

The solution of Eq. (1) is approximated by the cell averages $\bar{u}_i^n = \frac{1}{\Delta x} \int_{C_i} u(x, t^n) dx$ which are updated with the finite volume (FV) formulation of Eq. (1) given by

$$(2) \quad \frac{d\bar{u}_i}{dt} = -\frac{1}{\Delta x} \left(\hat{f}_{i+1/2} - \hat{f}_{i-1/2} \right).$$

The numerical flux function $\hat{f}_{i\pm 1/2} = f(u(x_{i\pm 1/2}, t))$ results from Eq. (1) by integrating over C_i . The aim is to define an update rule for the new time step $t^{n+1} = t^n + \Delta t$ such that Eq. (1) is approximated with high order of accuracy. The main challenge is to avoid the development of spurious oscillations near shocks and at the same time maintain high order accuracy at smooth extrema.

We are interested in a numerical scheme with the most compact stencil, using only information of the cell C_i and its most direct neighbors C_{i-1} and C_{i+1} . Classical approaches based on this three-point-stencil, such as the MUSCL scheme, yield 2nd order schemes [8, 5], however, we will present an update rule that yields 3rd order accuracy for smooth solutions.

The key point is the definition of the numerical flux function \hat{f} which depends on the left and right limiting values $u^{(\pm)}(x_{i\pm 1/2})$ at the cell boundaries $x_{i\pm 1/2}$, cf. Fig 1. These values are a priori not known and have to be reconstructed from the cell mean values \bar{u}_i^n . The focus of this work is on the reconstruction procedure.

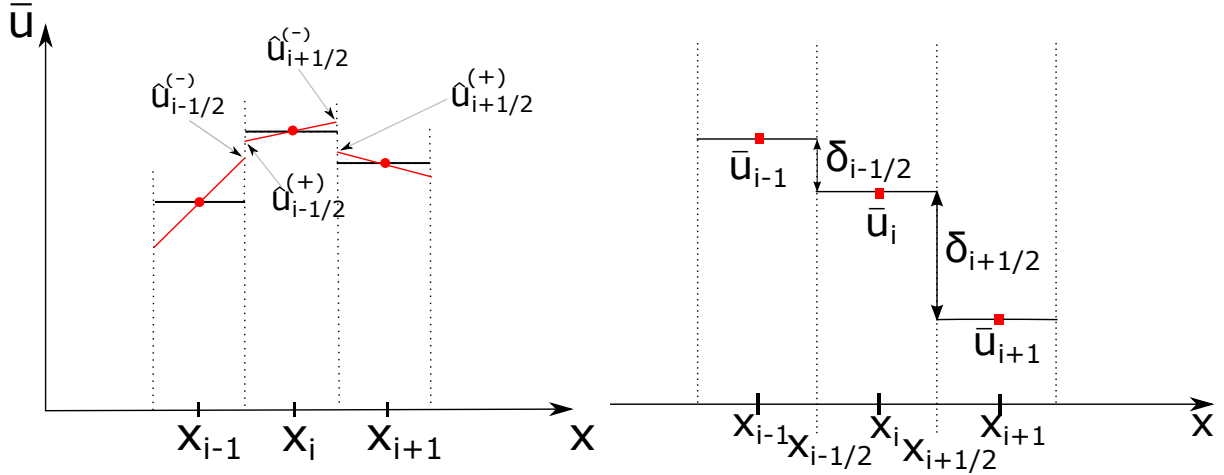


Figure 1. Basic setting for the reconstruction of the interface values $u^{(\pm)}(x_{i\pm 1/2})$ on a 3-point-stencil.

2. Theory

2.1. Two Parameter Setting

Considering the compact stencil $\{x_{i-1}, x_i, x_{i+1}\}$, we want to reconstruct the interface values at the cell boundaries $x_{i\pm 1/2}$ as shown in Fig. 1. For the cell x_i , we use the left and right interface values defined by

$$(3a) \quad u_{i+1/2}^{(-)} = \bar{u}_i + \frac{1}{2} \phi(\theta_i) \delta_{i+1/2}$$

$$(3b) \quad u_{i-1/2}^{(+)} = \bar{u}_i - \frac{1}{2} \phi(\theta_i^{-1}) \delta_{i-1/2}.$$

Here, ϕ is a non-linear limiter function depending on the local smoothness measure

$$\theta_i = \frac{\delta_{i-1/2}}{\delta_{i+1/2}}, \quad \delta_{i+1/2} \neq 0$$

with $\delta_{i+1/2} = \bar{u}_{i+1} - \bar{u}_i$, $\delta_{i-1/2} = \bar{u}_i - \bar{u}_{i-1}$, cf. Fig. 1. In Eq. (3), the choice of $\phi(\theta_i)$ determines the order of accuracy of the reconstruction and therefore of the scheme.

There is a variety of schemes on the three-point stencil that obtain 2nd-order accuracy. These are the classical schemes, which use the information of the three cells to compute a linear reconstruction function, see e.g. [8]. Indeed, the second-order reconstruction $u_{i+1/2}^{(-)} = \bar{u}_i + \frac{\Delta x}{2} \left(\frac{\bar{u}_{i+1} - \bar{u}_{i-1}}{2\Delta x} \right)$ can be rewritten in form of Eq. (3) with the limiter function $\phi(\theta) = \frac{1+\theta}{2}$. This limiter function has the property that $\phi(\theta^{-1}) = \theta^{-1}\phi(\theta)$ holds and therefore, Eq. (3) can be reduced to the standard formulation

$$(4a) \quad u_{i+1/2}^{(-)} = \bar{u}_i + \frac{\Delta x}{2} \sigma_i$$

$$(4b) \quad u_{i-1/2}^{(+)} = \bar{u}_i - \frac{\Delta x}{2} \sigma_i,$$

with the downwind slope $\sigma_i = \phi(\theta)\delta_{i+1/2}$ (see e.g. [5]). The aim of this work is to introduce schemes which use the three-point stencil to achieve 3rd order accurate reconstructions of the cell-interface values. One possibility is to construct a quadratic polynomial $p_i(x)$ in each cell. Applying the computed polynomial to $x_{i\pm 1/2}$ yields the interface values

$$(5a) \quad u_{i-1/2}^{(+)} = p_i(x_{i-1/2})$$

$$(5b) \quad u_{i+1/2}^{(-)} = p_i(x_{i+1/2}).$$

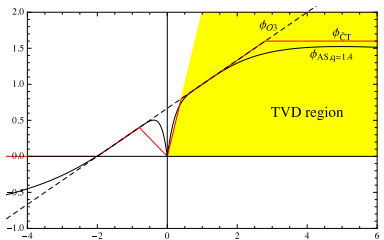


Figure 2. Alternative limiter matching the logarithmic limiter with $q = 1.4$.

Rewriting the interface values in the form (3) yields

$$(6) \quad \phi_{\mathcal{O}3}(\theta_i) = \frac{2 + \theta_i}{3}.$$

This formulation results in a full third order scheme for smooth solutions, however, causes oscillations near shocks and discontinuities. Since this should be avoided, we introduce a limiter function $\tilde{\phi}$, that applies the full 3rd order reconstruction Eq. (6) at smooth parts of the solution and switches to a lower order reconstruction formulation close to large gradients, shocks and discontinuities.

The limiting function we will dwell upon in this paper is based on the local double logarithmic reconstruction function of Artebrant and Schroll [1]. They present a limiter function $\phi_{AS}(\theta_i, q)$ which contains an additional parameter $q < 1$. This parameter significantly changes the reconstruction function. The authors state that $q = 1.4$ is the best choice and for $q \rightarrow 0$, the logarithmic limiter function reduces to $\phi_{\mathcal{O}3}(\theta_i)$, Eq. (6).

$$\phi_{AS}(\theta_i, q) = \frac{2p[(p^2 - 2p\theta + 1)\log(p) - (1 - \theta)(p^2 - 1)]}{(p^2 - 1)(p - 1)^2},$$

$$p = p(\theta_i, q) = 2 \frac{|\theta_i|^q}{1 + |\theta_i|^{2q}}.$$

The drawback of $\phi_{AS}(\theta_i, q)$ is its complexity which makes the evaluation in each cell expensive and possibly instable.

In [2], Čada and Torrilhon develop a limiter function $\phi_{\text{Lim}\mathcal{O}3}(\theta_i)$ that resembles the properties of ϕ_{AS} and reduces the computational cost. The alternative limiter function reads

$$\phi_{\text{Lim}\mathcal{O}3}(\theta_i) = \max \left(0, \min \left(\phi_{\mathcal{O}3}(\theta_i), \max \left(-\frac{1}{2}\theta_i, \min(2\theta_i, \phi_{\mathcal{O}3}(\theta_i), 1.6) \right) \right) \right)$$

and is shown in Fig. 2 together with $\phi_{AS}(\theta_i, 1.4)$ and $\phi_{\mathcal{O}3}(\theta_i)$.

All reconstruction functions presented so far have non-zero values for $\theta < 0$, which means that they break with the total variation diminishing (TVD) property. The idea of keeping the non-zero part in the construction of $\phi_{\text{Lim}\mathcal{O}3}(\theta)$ for $\theta \in [-2, 0]$ was to avoid the clipping of smooth extrema. Extrema clipping is the effect that occurs close to minima and maxima, where the normalized slopes $\delta_{i\pm 1/2}$ are of the same order of magnitude but have opposite signs, i.e. $\theta \approx -1$. In this case, classical limiter functions that fully lie in the TVD region yield zero and thus 1st order accuracy. This effect is avoided including the non-zero part in $\phi_{\text{Lim}\mathcal{O}3}$.

Another clipping phenomenon arises, if the discretization of a smooth function contains a zero slope, $\delta_{i-1/2} \approx 0$ or $\delta_{i+1/2} \approx 0$. This leads to $\theta \rightarrow 0$ or $\theta \rightarrow \pm\infty$ and the interface values are approximated by the cell mean values, which yields a 1st order scheme. This case shows, that we need a criterion that can differentiate between smooth extrema and discontinuities. We require this decision criterion to depend only on information available on the compact three-point stencil. Furthermore, it has to detect cases when to switch to the 3rd order reconstruction, Eq. (6), in case of smooth extrema, even though one of the normalized slopes is zero. This is the case if the non-zero slope is 'small', compared to the case of a discontinuity. The main focus of this work is to determine what 'small' means and to define a switch function η .

From the discussion above, it is clear that η has to explicitly depend on both normalized slopes $\delta_{i\pm 1/2}$. The classical approach of considering the ratio θ_i of neighboring slopes is overly restrictive because part of the information is given away. This is why we reformulate the limiter functions ϕ in a two-parameter-framework and obtain the new formulation for the reconstructed interface values

$$(7a) \quad u_{i+1/2}^{(-)} = \bar{u}_i + \frac{1}{2} \tilde{\phi}(\delta_{i-1/2}, \delta_{i+1/2}),$$

$$(7b) \quad u_{i-1/2}^{(+)} = \bar{u}_i - \frac{1}{2} \tilde{\phi}(\delta_{i+1/2}, \delta_{i-1/2}),$$

where the limiter function in the two-parameter framework is defined by

$$(8) \quad \tilde{\phi}(\delta_{i-1/2}, \delta_{i+1/2}) = \phi(\delta_{i-1/2}/\delta_{i+1/2})\delta_{i+1/2}.$$

This formulation avoids the division by the normalized slope which can be close to zero and thus cause instabilities.

In this setting, the full-third-order reconstruction, Eq. (6), reads

$$(9) \quad \tilde{\phi}_{\mathcal{O}3}(\delta_{i-1/2}, \delta_{i+1/2}) = \frac{2\delta_{i+1/2} + \delta_{i-1/2}}{3}.$$

Fig. 3a shows the alternative limiter function $\tilde{\phi}_{\text{Lim}\mathcal{O}3}$ and the full-third-order reconstruction $\tilde{\phi}_{\mathcal{O}3}$ in the two-parameter setting.

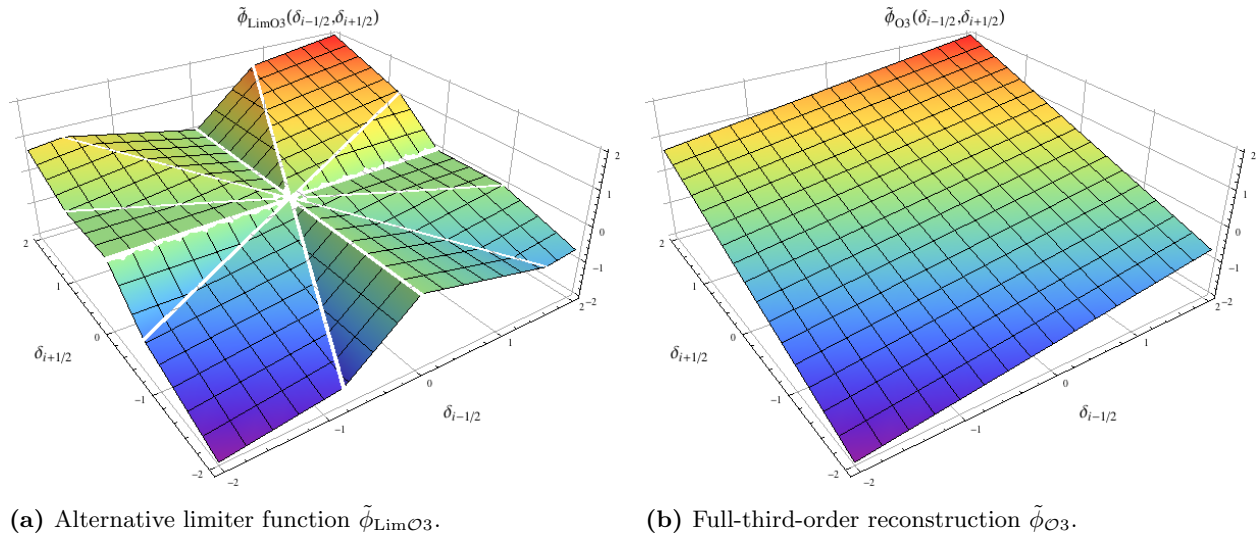


Figure 3. Different reconstruction functions in the two-parameter-framework.

On the coordinate axis, where $\delta_{i-1/2} = 0$, i.e. $\theta_i = 0$, the limiter function $\tilde{\phi}_{\text{Lim}\mathcal{O}3}$ returns zero, meaning that it yields a 1st order method. The same holds for the coordinate axis where $\delta_{i+1/2} = 0$, see Eq. (8). For two consecutive slopes of approximately the same order of magnitude, i.e. around the diagonals, the 3rd order reconstruction Eq. (9) is gained.

Note that the limiter function presented in [2] is not symmetric with respect to the diagonals. This means that for some cases $\tilde{\phi}_{\text{Lim}\mathcal{O}3}(\delta_1, \delta_2) = \tilde{\phi}_{\mathcal{O}3}(\delta_1, \delta_2)$ but $\tilde{\phi}_{\text{Lim}\mathcal{O}3}(-\delta_2, -\delta_1) \neq \tilde{\phi}_{\mathcal{O}3}(-\delta_2, -\delta_1)$, cf. Fig. 4. This should not be the case. We therefore corrected this feature and defined the resulting limiter function $\tilde{\phi}_{\text{new}}$,

$$\begin{aligned} \tilde{\phi}_{\text{new}}(\delta_{i-1/2}, \delta_{i+1/2}) &= \phi_{\text{new}}(\theta_i) \delta_{i+1/2}, \\ \phi_{\text{new}}(\theta_i) &= \max\left(0, \min\left(\tilde{\phi}_{\mathcal{O}3}, \max\left(-\theta_i, \min\left(2\theta_i, \tilde{\phi}_{\mathcal{O}3}, 1.5\right)\right)\right)\right). \end{aligned}$$

This new limiter function treats symmetric situations in the same manner, i.e. if $\tilde{\phi}_{\text{new}}(\delta_1, \delta_2) = \tilde{\phi}_{\mathcal{O}3}(\delta_1, \delta_2)$ then also $\tilde{\phi}_{\text{new}}(-\delta_2, -\delta_1) = \tilde{\phi}_{\mathcal{O}3}(-\delta_2, -\delta_1)$.

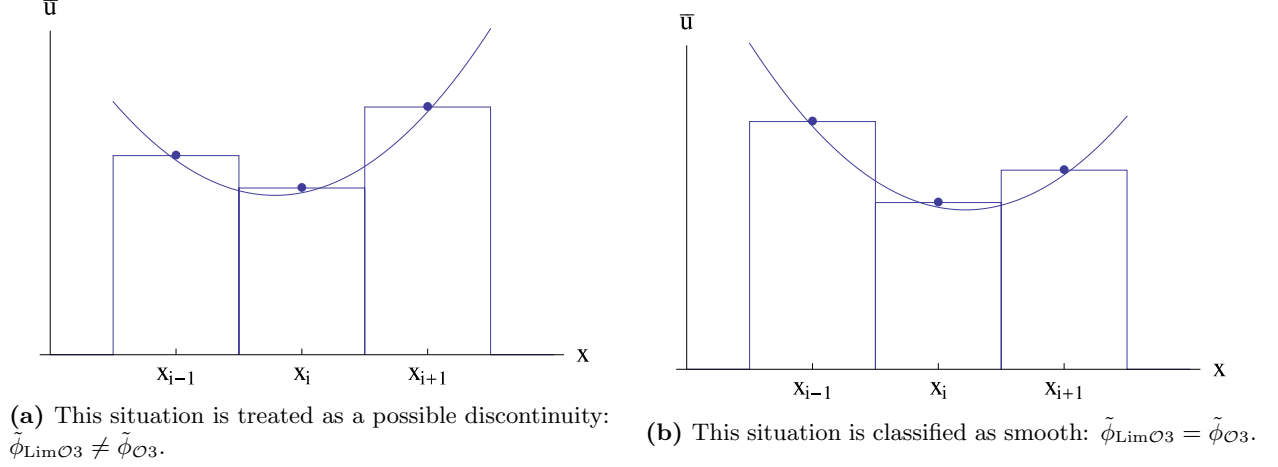


Figure 4. Two similar situations that are treated differently by $\tilde{\phi}_{\text{Lim}\mathcal{O}3}$.

2.2. Decision Criterion

On a three-point stencil, it is almost impossible to define a criterion that fully ascertains whether the function exhibits the beginning of a discontinuity or a smooth extremum. As stated in Sec. 2.1, the two-parameter setting is the necessary prerequisite for the definition of such a criterion. In an earlier work [2], Čada and Torrilhon proposed a switch function $\eta(\delta_{i-1/2}, \delta_{i+1/2})$ which tests for smooth extrema. Their switch function defines an asymptotic region of radius r around the origin in the $\delta_{i+1/2} - \delta_{i-1/2}$ - plane in which we can safely switch to the third-order scheme. The limiter function $\phi_{\text{Lim}\mathcal{O}3}$ together with this switch function has been successfully applied (e.g. [3, 4, 6, 7]). Unfortunately, the authors do not specify the parameter r , which determines the size of the asymptotic region. With this idea in mind, we found that the most promising potential to distinguish discontinuities from smooth extrema is by measuring the magnitude of the vector $(\delta_{i-1/2}, \delta_{i+1/2})$. When this vector is bounded in some appropriate norm, the reconstruction is switched to the full-third-order reconstruction, even though one of lateral derivatives may be vanishing.

Lemma 2.1. *In the vicinity of an extremum ξ_0 , for $|x_i - \xi_0| \leq \Delta x$, the following relations hold:*

$$(10a) \quad \left\| \begin{pmatrix} \delta_{i-1/2} \\ \delta_{i+1/2} \end{pmatrix} \right\|_2 \leq c \max_i |u''_{0i}| \Delta x^2 \quad \text{with } c = \sqrt{\frac{5}{2}}$$

$$(10b) \quad \left\| \begin{pmatrix} \delta_{i-1/2} \\ \delta_{i+1/2} \end{pmatrix} \right\|_1 \leq c \max_i |u''_{0i}| \Delta x^2 \quad \text{with } c = 2$$

Lemma 2.1 makes a statement on the magnitude of the differences across the cell interfaces. The bound only depends on the grid size Δx and the initial condition u_0 .

Definition 2.2. *The switch function η that marks the limit between smooth extrema and discontinuities is defined by*

$$(11) \quad \eta = \frac{\sqrt{\delta_{i-1/2}^2 + \delta_{i+1/2}^2}}{\sqrt{\frac{5}{2}} \alpha \Delta x^2} \leq 1$$

with

$$(12) \quad \alpha \equiv \max_{i \in \Omega \setminus \Omega_d} |u''_{0i}(x)|.$$

Here, Ω is the computational domain and Ω_d is a set of points where the initial condition u_0 is discontinuous.

Proof. (Proof of Lemma 2.1)

Eq. (10a) can be proven using a similar formulation of Def. 2.2:

$$(13) \quad \frac{\delta_{i-1/2}^2 + \delta_{i+1/2}^2}{(\alpha \Delta x^2)^2} = \frac{1}{\alpha^2} \left(\frac{u_{i+1} - 2u_i + u_{i-1}}{\Delta x^2} \right)^2 + \frac{2}{\alpha^2 \Delta x^2} \left(\frac{u_{i+1} - u_i}{\Delta x} \right) \left(\frac{u_i - u_{i-1}}{\Delta x} \right)$$

A Taylor development around x_i yields

$$(14) \quad \frac{\delta_{i-1/2}^2 + \delta_{i+1/2}^2}{(\alpha \Delta x^2)^2} = \frac{1}{2} \left(\frac{u_i''}{\alpha} \right)^2 + \frac{2}{\Delta x^2} \left(\frac{u_i'}{\alpha} \right)^2 + \frac{5}{6} \frac{u_i' u_i^{(3)}}{\alpha^2} + \mathcal{O}(\Delta x^2).$$

In the vicinity of an extremum ξ_0 , for $|x_i - \xi_0| \leq \Delta x$, the derivative fulfills $u_i' \leq u_{\xi_0}'' \Delta x + \mathcal{O}(\Delta x^2)$. Therefore, Eq. (14) reduces to

$$(15) \quad \frac{\delta_{i-1/2}^2 + \delta_{i+1/2}^2}{(\alpha \Delta x^2)^2} \leq \frac{1}{2} \left(\frac{u_i''}{\alpha} \right)^2 + 2 \left(\frac{u_{\xi_0}''}{\alpha} \right)^2 + \mathcal{O}(\Delta x).$$

Setting $\alpha \equiv \max_{i \in \Omega \setminus \Omega_d} |u_{0_i}''(x)|$

$$\frac{\delta_{i-1/2}^2 + \delta_{i+1/2}^2}{(\alpha \Delta x^2)^2} \leq \frac{5}{2}$$

holds true, which shows Eq. (10a).

In a similar manner, Eq. (10b) can be proven. \square

With Def. 2.2, Lemma 2.1 states that in the vicinity of smooth extrema, $\eta \leq 1$ holds. Combining this information with the new limiter function $\tilde{\phi}_{\text{new}}$, we use this result to define the combined limiter

$$\tilde{\phi}_{\text{comb}}(\delta_{i-1/2}, \delta_{i+1/2}) := \begin{cases} \tilde{\phi}_{\mathcal{O}3}(\delta_{i-1/2}, \delta_{i+1/2}) & \text{if } \eta < 1 - \varepsilon \\ \tilde{\phi}_{\text{new}}(\delta_{i-1/2}, \delta_{i+1/2}) & \text{if } \eta > 1 + \varepsilon \\ W(\tilde{\phi}_{\mathcal{O}3}, \tilde{\phi}_{\text{new}}) & \text{else.} \end{cases}$$

where ε is a small number of order 10^{-6} and $W(\cdot, \cdot)$ a linear function to ensure Lipschitz continuity of $\tilde{\phi}_{\text{comb}}$, cf. [2] for more details.

3. Numerical Results

In this section we want to test the decision criterion η for the one-dimensional linear advection equation

$$(16a) \quad u_t + u_x = 0,$$

$$(16b) \quad u(x, t = 0) = u_0(x),$$

with two different characteristic initial conditions (ICs) on a periodic domain $[-1, 1]$. Since η requires the input of $\alpha = \max_{i \notin \Omega_d} |u_{0_i}''|$ this external input is a possible source of error. For this reason, we test for input values that are

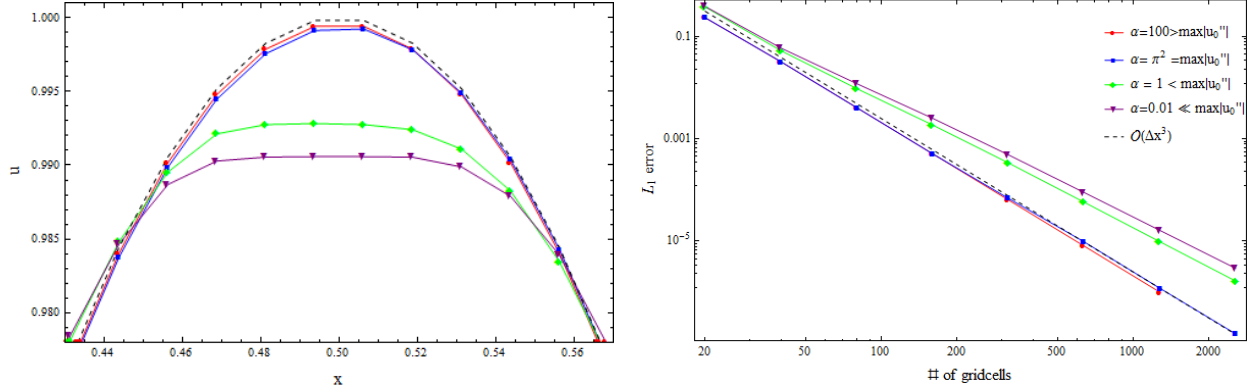
- (1) of the right order of magnitude
- (2) over estimated, i.e too large
- (3) under estimated, i.e. too small
- (4) much too small.

The aim is to study the impact of possibly-incorrect input values and thus wrong switching functions η .

3.1. Convergence Studies For Smooth Initial Data

We solve the advection equation (16) with the IC $u_0(x) = \sin(\pi x)$, $x \in [-1, 1]$. The function is convected until $t_{\text{end}} = 20$ with Courant number $\nu = 0.8$. In Fig. 5a we have plotted an area of interest of the solution of Eq. (16). Fig. 5b shows the double-logarithmic L_1 -error vs. number of grid cells. Both plots are depicted for different values of α and have been calculated for $n = 160$ grid cells, i.e. $\Delta x = 0.0125$.

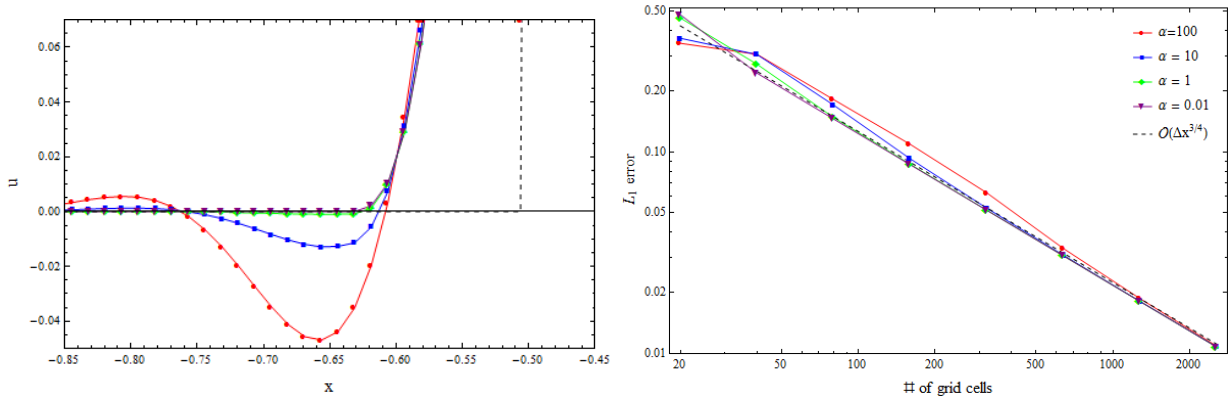
Fig. 5 clearly points out that for the smooth test case, an over estimation of α does not effect the 3rd-order convergence of the solution. This is due to the fact that a large α means essentially no limiting but a direct

(a) Solution of Eq. (16) for different values of α .(b) Double-logarithmic plot of the L_1 -error vs. number of grid cells.**Figure 5.** Results are calculated at $t_{\text{end}} = 20.0$ using $u_0(x) = \sin(\pi x)$, $\nu = 0.8$, $\Delta x = 0.0125$.

application of the full 3rd-order reconstruction. If the input value for α is smaller, the limiter function $\tilde{\phi}_{\text{new}}$ is applied more often. In this case, a higher resolution is needed to distinguish between the discretization of a smooth extremum and a shallow gradient.

3.2. Initial Condition with Discontinuous Data

In case of the square wave $u_0(x) = \mathbb{1}_{[-0.5, 0.5]}(x)$, $x \in [-1, 1]$, the input for α , as defined by Eq. (12) would yield 0. However, this means that the new limiter function $\tilde{\phi}_{\text{new}}$ always takes effect and yields 0 in most parts of the domain. This is because at least one of the consecutive slopes $\delta_{i\pm 1/2} = 0$. However, arguing that in the smooth parts, $\delta_{i+1/2} \approx \delta_{i-1/2}$ (even though they yield 0), we are close to the diagonals and thus, the 3rd-order reconstruction should be applied. Testing different values of α revealed that for larger values, the

(a) Solution of Eq. (16) for different values of α .(b) Double-logarithmic plot of the L_1 -error vs. number of grid cells.**Figure 6.** Results are calculated at $t_{\text{end}} = 20.0$ using $u_0(x) = \mathbb{1}_{[-0.5, 0.5]}(x)$, $\nu = 0.8$, $\Delta x = 0.0125$.

oscillatory behavior increases. This is due to the fact that with increasing α the region where $\tilde{\phi}_{\mathcal{O}3}$ is applied increases. Utilizing solely the full 3rd-order reconstruction $\tilde{\phi}_{\mathcal{O}3}$ on the square wave is known to result in large over- and undershoots and to asymptotically yield order $\mathcal{O}(\Delta x^{3/4})$. Fig. 6 shows that for small values of α , the solution converges faster to $\mathcal{O}(\Delta x^{3/4})$ than for large values of α . Thus, small values should be preferred, however, even when the input for α is overestimated, the solution converges when a sufficient number of grid cells is used.

References

- [1] Artebrant, R. and Schroll, H.J. (2005). *Conservative logarithmic reconstructions and finite volume methods*. SIAM Journal on Scientific Computing, 27(1), 294-314.
- [2] Čada, M. and Torrilhon, M. (2009). *Compact third-order limiter functions for finite volume methods*. Journal of Computational Physics, 228(11), 4118-4145.
- [3] Kemm, F. (2011). *A comparative study of TVD-limiters – well-known limiters and an introduction of new ones*. International Journal for Numerical Methods in Fluids, 67(4), 404-440.
- [4] Keppens, R. and Porth, O. (2014). *Scalar hyperbolic PDE simulations and coupling strategies*. Journal of Computational and Applied Mathematics, 266, 87-101.
- [5] LeVeque, R. J. (2002). *Finite Volume Methods for Hyperbolic Problems*. Cambridge University Press.
- [6] Mignone, A., Tzeferacos, P., and Bodo, G. (2010). *High-order conservative finite difference GLM-MHD schemes for cell-centered MHD*. Journal of Computational Physics, 229(17), 5896-5920.
- [7] Porth, O., Komissarov, S. S., and Keppens, R. (2014). *Three-dimensional magnetohydrodynamic simulations of the Crab nebula*. Monthly Notices of the Royal Astronomical Society, 438(1), 278-306.
- [8] Van Leer, B. (1979). *Towards the ultimate conservative difference scheme V: A second-order sequel to Godunov's method*. Journal of computational Physics, 32(1), 101-136.

^{a)} CENTER FOR COMPUTATIONAL ENGINEERING SCIENCE
RWTH AACHEN UNIVERSITY
D-52062 AACHEN
GERMANY
E-mail address: `schmidtmann@mathcces.rwth-aachen.de`

^{b)} INSTITUT FÜR MATHEMATIK & COMPUTATIONAL SCIENCE
UNIVERSITÄT ZÜRICH
CH-8057 ZÜRICH
SWITZERLAND
E-mail address: `remi.abgrall@math.uzh.ch`